

# The optimal branching asymmetry of a bidirectional distribution tree

M. Florens<sup>a,\*</sup>, B. Sapoval<sup>b,a</sup>, M. Filoche<sup>b,a</sup>

<sup>a</sup>CMLA, ENS Cachan, CNRS, UniverSud, 61 Avenue du Président Wilson, F-94230 Cachan, France

<sup>b</sup>Physique de la Matière Condensée, Ecole Polytechnique, CNRS, 91128 Palaiseau Cedex, France

---

## Abstract

Several transportation networks in living systems are pulsatile branching trees. Due to the alternating character of the flow, these trees have to simultaneously satisfy two constraints: they have to deliver the carried products in a limited time and they must exhibit a satisfactory aerodynamic performance in both directions of the flow. We report here that introducing a systematic branching asymmetry into a distribution tree improves performance and robustness, both at inhalation and exhalation. Moreover, optimizing the asymmetry level for both phases leads to a value very close to the one measured in the human lung.

*Keywords:* tracheobronchial tree, branching asymmetry, compliant airway, pulsatile flow, optimal transport

*PACS:* 87.19.Wx, 47.60.Dx, 89.75.Fb

---

## 1. Introduction

Numerous biological transportation networks are branching trees. One can distinguish several types of trees depending on the nature of the flow that crosses them: it can be a unidirectional stationary flow, as in the case of the vascular venous system in mammals, or a unidirectional pulsatile flow, as in the vascular arterial system, or a bidirectional flow. A striking example of the last case is provided by the mammalian pulmonary airway system in which the air flow undergoes periodic oscillations: in humans, during each breathing cycle, air enters the system during 2 seconds at rest in order to deliver oxygen to the gas exchange units located in the distal regions (the *acini*). During expiration (3 seconds at rest), air flows out to clear the carbon dioxide brought by the venous system. Due to the alternate character of the flow, such a system has to simultaneously be able to deliver the carried products in a limited time, and to present a limited aerodynamic resistance in both directions of the flow.

The geometrical structure of the human pulmonary airway system is that of a dichotomous branching tree. At each bifurcation, the parent branch gives rise to two daughter branches which belong to a new generation [1, 2]. The total number of generations depends on the pathway in the tree and is about 23 on average in the human lung. From the physiological point of view, the airway system can be schematically subdivided into two subsystems: first, the *tracheobronchial tree* which is a purely conducting tree. It starts at the trachea (generation 0) whose average diameter and length are respectively  $D=1.8$  cm and  $L=12$  cm in the healthy human adult. It ends in the terminal bronchioles whose average diameter is about 0.5 mm. These terminal bronchioles are located on average around generation

15 [3]. Second, from the terminal bronchioles start the *acini* which are the gas exchange units between air and blood. We will from now focus only on the first subsystem, the tracheobronchial tree.

One very interesting geometrical feature of this tree is its branching asymmetry. This means that, at every generation, each parent airway gives rise to a larger daughter airway (the major airway) and a smaller daughter airway (the minor airway). This asymmetry has been extensively measured [3] and analyzed [4]. The goal of this article is to study in a realistic model of the human airway system the influence of this branching asymmetry on the ventilation performance of the human lung, both at inhalation and exhalation.

## 2. The geometrical model of the tracheobronchial tree

Regarding gas transport, the tracheobronchial tree can essentially be modeled as an arrangement of cylindrical pipes defined by their diameter and length. A fundamental step in describing its morphology has been the introduction of the now classical symmetric Weibel's A model [1]. In the simplest version of this model, the tree is likened to a hierarchical network of pipes with symmetrical dichotomous branching and a uniform scaling ratio,  $h_0 = 2^{-1/3} \approx 0.79$  between the airway diameters of consecutive generations. However, in order to account for the distribution of the airway sizes at any given generation, one has to introduce a systematic branching asymmetry at every bifurcation [2, 4]. This branching asymmetry can be characterized by two different scaling ratios,  $h_{0\max}=0.88$  and  $h_{0\min}=0.68$ . For proximal airways (generations 1 to 4), morphometric measurements show that their sizes significantly deviate from a general scaling [1, 5, 6, 4] and require specific parameters.

The geometrical model of the tracheobronchial tree used in this study therefore consists in a set of specific parameters for the first generations, and relies on systematic scaling and

---

\*Magali Florens, CMLA, Ens Cachan, 61 Avenue du Président Wilson, F-94230 Cachan, France, Tel : +33(0)169334699, Fax : +33(0)169334799.

branching asymmetry in the intermediate bronchial tree. This model, characterized by the parameters in Tab. 1, allows to reproduce the airway size distributions as measured in the literature. Since all terminal bronchioles have essentially comparable diameters (about 0.5 mm) [7, 8], the branching asymmetry implies that different pathways starting at the trachea and finishing in a terminal bronchiole may have different number of generations. The generation number of the terminal airways range from 8 to 22 in the human lung [5, 3].

Generation	Scaling ratio for $D$		Ratio $L/D$
	$h_{0\ max}$	$h_{0\ min}$	
1	0.88	0.68	3.07
2	0.88	0.68	1.75
3	0.88	0.68	1.43
4	0.88	0.68	1.85
$\geq 5$	0.88	0.68	3.00

Table 1: Parameters of the geometrical tracheobronchial tree model.  $D$  and  $L$  represent airway diameter and length.

### 3. Inhalation

We first study the ventilation performance of the bronchial tree. The criterion used to characterize this performance is the distribution of the oxygenation times of the acini. For each acinus, the oxygenation time is defined as the duration during which fresh air is delivered to it at inhalation. It is computed by subtracting from the total duration of the inspiratory phase,  $t_{ins}$  (2 s), the time spent in the extrathoracic airways,  $t_{ext}$  (approximately constant and equal to 0.47 s at rest [9]), and the transit time from the trachea to the acinus,  $t_{tr}$ :

$$t_{ox} = t_{ins} - t_{ext} - t_{tr}$$

Each acinus is assumed to act as an hydrodynamic pump draining the same flow. As a consequence, starting from the bottom of the tree, the flow can be computed in each airway. The time spent in an airway is directly obtained from the flow rate and airway sizes. The total flow rate is considered approximately constant during the entire inspiratory phase, with a velocity in the trachea of about 1 m/s [7]. The total transit time from the trachea to a terminal bronchiole is thus determined by the sum of the times to cross each branch of the pathway leading to this terminal bronchiole. This transit time has to be as small as possible to provide an efficient ventilation of the acinus.

Using our asymmetric model, we compute the distribution of oxygenation times in all acini. They are spread around an average value  $t_{ox} = 0.67$  s with a standard deviation of about 0.13 s. All acini are thus found to receive fresh air during inspiration since all transit times are smaller than  $t_{ins} - t_{ext} = 1.53$  s.

We now address the question of the robustness of this ventilation performance against anatomical variability. To account for this variability, the scaling ratios are randomized: at each bifurcation, the major and minor scaling ratios,  $h_{max}$  and  $h_{min}$ , are

now anticorrelated random variables, so that the Hess-Murray law still holds:

$$h_{max}^3 + h_{min}^3 = 1,$$

Their average value is determined by the parameters in Tab. 1 and their standard deviation is taken equal to 0.10 [4]. As a consequence, all diameters and lengths are also random variables. Computing the distribution of oxygenation times in this randomized tree, one obtains almost exactly the same result as for the deterministic model. The asymmetric bronchial tree thus appears to have an efficient ventilation performance which is also robust against morphological variability.

Branching asymmetry tends to spread the distribution of oxygenation times. Wider pathways in the tree are associated to larger transit times due to flow conservation. If the asymmetry is too large, the transit time in some pathways will increase to a value close to the duration of inhalation. One can therefore ask the following question: is there a threshold asymmetry level above which some acini do not receive fresh air at all? To answer this question, we introduce a parameter  $\alpha$  which characterizes the asymmetry level. This parameter is defined as followed:

$$\begin{aligned} h_{0\ max}^3 &= h_0^3 (1 + \alpha) \\ h_{0\ min}^3 &= h_0^3 (1 - \alpha) \end{aligned}$$

The asymmetry level measured in the human lung corresponds to a value of about 36% ( $h_{0\ max} = 0.88$  and  $h_{0\ min} = 0.68$ ). Thanks to the definition of  $\alpha$ , all bronchial trees built using such rules have the same thoracic volume. Moreover, they have the same specific values of the ratio  $L/D$  for the first generations (Tab. 1), and the threshold diameter that determines the terminal bronchiole is identical.

Numerical computations of the oxygen transport, achieved by solving time dependent equations of diffusion and convection in the acinus geometry, have shown that fresh air has to remain at least 0.3 s in the acinus in order to achieve the gas exchange process [10]. We have therefore computed for each asymmetry level the number of acini which have an oxygenation time smaller than 0.3 s. In other words, these acini do not permit the oxygen transfer between air and blood (Fig. 1). They are called *unactive* acini.

It is found that all acini are supplied with fresh air (which means 0% of unactive acini) when the asymmetry level is smaller than a critical threshold value which is about 35%. Above this value, the number of acini unable to transfer oxygen to the blood during inspiration significantly rises. Interestingly, this threshold value almost exactly corresponds to the branching asymmetry level measured in the human lung ( $\alpha=36\%$ ). It has already been reported in a previous article that branching asymmetry contributes to reduce the aerodynamic resistance of the tree in the Poiseuille flow approximation [11]. This first study at inhalation seems to indicate that evolution has adjusted the asymmetry level at its maximum value allowing to feed all terminal units with fresh air.

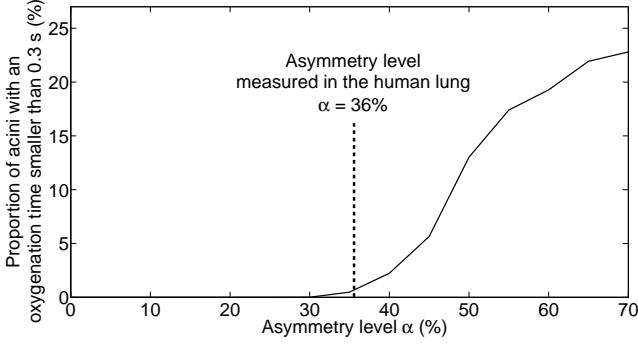


Figure 1: Proportion of unactive acini (with oxygenation time smaller than 0.3 s) as a function of the asymmetry level  $\alpha$ .

#### 4. Forced Expiration

At expiration, the total quantity of the air previously inhaled has to be exhaled in a limited time in order to renew it with fresh air. However, exhalation is not the symmetric counterpart of inhalation: due to the pressure exerted by the diaphragm and the elastic energy stored in the respiratory muscles, the compliant properties of the airways now play a major role. The flow pattern in the tree is then the result of a complex interplay between the flexible airway structure and the applied pressure distribution. In extreme conditions, as in forced expiration, the system exhibits non linearities that may lead to important inhomogeneities in the flow distribution.

In particular, forced expiration maneuvers can be seen as a signature of the behavior of the compliant bronchial geometry. This explains why they have been used for many years to test lung function [12]. During these maneuvers, the most common procedure consists in recording the maximal expiratory flow-volume (MEFV) curves. To assess the role of branching asymmetry at exhalation, we have simulated these curves using a 1D model in each branch of the bronchial tree.

Two fundamental equations are used to describe the mechanical behavior of an individual airway at expiration.

First, the airway compliance is modeled using Lambert's equations [13] which relate the local airway diameter  $D$  to the local transmural pressure  $P$ , the latter being the difference between the internal airway pressure and the external pleural pressure assumed uniform. We also assume that all airways are intrapleural excepted the trachea that is treated as semi-intrathoracic. In Lambert's model, the parameters are defined for each generation. In the asymmetric tree, this cannot be done as such since airways of very different diameters and compliances can be found at the same generation. We therefore introduce a generalized version of this model in which Lambert's parameters do not depend on airway generation but on airway diameter. The pleural pressure is taken equal to the difference between the alveolar pressure and the static recoil pressure. Both pressures are modeled according Polak's model [14]. The alveolar pressure depends on patient's effort through the maximal expiratory pressure  $P_m$  and the time constant of the expiratory muscles  $\tau$ .

Second, the gradient of transmural pressure  $dP/dx$  along the airway is computed using the 1D model introduced by Lambert et al. for a steady and incompressible flow [13]:

$$\frac{dP}{dx} = \frac{-f}{1 - \frac{v^2}{c^2}} = \frac{-f}{1 - \frac{2v^2\rho}{D} \left( \frac{dD}{dP} \right)}, \quad (1)$$

Here,  $f$  is the dissipative pressure loss per unit distance,  $D$  is the local airway diameter,  $v$  is the local flow velocity,  $c$  is the local wave speed, and  $\rho$  is the air density. It has to be noted that  $f$ ,  $D$ ,  $v$ , and  $c$  all vary along the airway. The local dissipative pressure loss  $f(x)$  is linked to the diameter  $D$  by:

$$f(x) = \frac{128\eta\Phi}{\pi D^4} (1.5 + 0.0035 Re) \quad (2)$$

where  $\eta$  is the air viscosity,  $\Phi$  the flow in the airway, and  $Re$  is the Reynolds number [15].

One of the important features appearing in these MEFV curves is *expiratory flow limitation* (EFL) [16]. Several mechanisms are responsible for EFL: first, the wave-speed mechanism introduced by Dawson and Elliot in 1977 [17]. The fluid velocity cannot be larger than the propagation speed  $c$  of pressure waves along the airway wall. Indeed, one can see in equation (1) that the pressure gradient  $dP/dx$  dramatically increases when the fluid velocity is close to the wave speed. The second mechanism responsible for EFL is a combination of the viscous loss of pressure and of the pressure loss due to convective acceleration [18].

Modeling forced expiration in the entire tree is computationally complex: it requires to numerically solve in *each airway* the differential equation (1) using expression (2) for  $f$ . This is usually achieved by numerical integration [13, 14, 19]. All these equations are coupled by flow continuity equations at each bifurcation of the tree, the pressure drops at the bifurcation being assumed here to be negligible [19]. On total, this means solving about 60,000 coupled highly non linear differential equations, at each time step of the expiration [13, 14]. For that reason, previous studies have simplified the tree geometry in order to reduce the number of differential equations, the symmetric Weibel's A model being there the most popular model used [13, 20]. All airways are thus assumed to be identical at each generation. Computing the flow in the entire tree at forced expiration comes down to numerically integrate 15 equations, one for each generation.

We show here that in fact, equation (1) can be exactly integrated assuming that the average Reynolds number along an airway can be estimated from its values at both ends of the airway:

$$\langle Re \rangle = \frac{4\rho\Phi}{\eta\pi \left( \frac{D_{in} + D_{out}}{2} \right)} \quad (3)$$

$D_{in}$  and  $D_{out}$  are the inlet and outlet airway diameters. Equation (1) therefore rewrites:

$$\frac{dP}{dx} = - (1.5 + 0.0035 \langle Re \rangle) \frac{8\pi\eta\Phi}{\frac{\pi^2}{16} D^4 - \Phi^2 \frac{2\rho}{D} \frac{dD}{dP}} \quad (4)$$

Since  $\langle Re \rangle$  and  $\Phi$  are constant along the airway, the only varying quantities are  $P$  and  $D$ . This differential equation can then be exactly integrated along the airway:

$$\frac{\pi^2}{16} \int_{in}^{out} D^4(P) dP - 2\rho \Phi^2 \int_{in}^{out} \frac{dD}{D} = - (1.5 + 0.0035 \langle Re \rangle) \times 8\pi\eta \int_{in}^{out} \Phi dx \quad (5)$$

which also writes:

$$\frac{\pi^2}{16} (g(P_{out}) - g(P_{in})) - 2\rho \Phi^2 \ln\left(\frac{D_{out}}{D_{in}}\right) = - (1.5 + 0.0035 \langle Re \rangle) 8\pi\eta \Phi L \quad (6)$$

where  $P_{in}$  and  $P_{out}$  are the transmural pressures at the airway inlet and outlet and  $L$  is the airway length. The function  $g(P)$  is determined by the relation between the airway diameter and the transmural pressure [13] and is defined as follows:

$$g(P) = \int_0^P D^4(P') dP' \quad (7)$$

Moreover, it has to be underlined that in the case of the Lambert's model of collapsible airways [13], this function  $g(P)$  can also be integrated analytically. For a different model, it might be necessary to tabulate it. In all cases, thanks to the expression obtained in equation (6), computing the pressures and diameters in the entire tree now only requires to solve about 60,000 coupled non linear *scalar* equations, which is a feasible goal.

To compute forced expiration, one imposes the atmospheric pressure at the top of the tree and an identical pressure, the alveolar pressure at all outlets of the tree. In the computations shown here, we restrain ourselves to trees of 13 generations on average. This is equivalent to assume that the pressure at the outlet of airways of generation 13 is about the same as the alveolar pressure, the airflow resistance of peripheral airways being small compared to that of the central airways [12]. This assumption can be generalized to an asymmetric tree: the pressure at the outlet of airways with a diameter equal to the average diameter of airways of generation 13 is the alveolar pressure. For the extrathoracic airways, the pressure drop is calculated using [14].

We use a quasi-static approach which means that a steady-state flow is computed in the entire tree at each time step of the exhalation. The entire non linear system, whose unknowns are the pressures  $P_{in}$  and  $P_{out}$ , and the flow  $\Phi$  in each airway, is solved using Newton-Raphson technique. Once the system is solved for a given time step, new conditions (lung volume, alveolar pressure, elastic lung recoil, pleural pressure) are applied and new flows are calculated in the entire bronchial tree. Time steps are by default 0.01 s and are adapted in order to obtain a stable solution.

We have studied here two different geometrical models of the bronchial tree, one symmetric and one asymmetric. The symmetric bronchial tree model is obtained using Tab. 1; the symmetric model is obtained from the exact symmetrization of the asymmetric one using at each bifurcation a single scaling ratio

$h_0$  defined by:  $h_0^3 = (h_{0\max}^3 + h_{0\min}^3)/2$ . Such a symmetrization allows to keep the same dead space volume (i.e. the inner tracheobronchial volume) for both geometrical models. In both cases, the fixed airway diameters thus obtained are used as maximal airway diameters that enter the relations  $D(P)$  from Lambert's model. The airway lengths are assumed to be constant during forced expiration and equal to the lengths computed by the geometrical model.

Fig. 2 (left) presents the simulated flow-volume curves for various patients' efforts in the asymmetric tree. In our model, the effort intensity modifies the maximal expiratory pressure  $P_m$  and the time constant of the expiratory muscles  $\tau$  which determine the alveolar pressure:  $P_m$  and  $\tau$  decrease when the patient's effort decreases. As we can see on Fig. 2, the first parts in all curves are effort dependent: the peak flow increases for larger effort. On the other hand, the second parts are effort independent: above a given expired volume, air flow does not increase when increasing the driving pressure. Our model reproduces both characteristic parts of the MEFV curves, in good agreement with classical measurements [16, 12]. Fig. 2 (right) is a comparison of MEFV curves for both symmetric and asymmetric tree structures. One can observe that branching asymmetry does not seem to have any influence on the MEFV curves in a healthy bronchial tree.

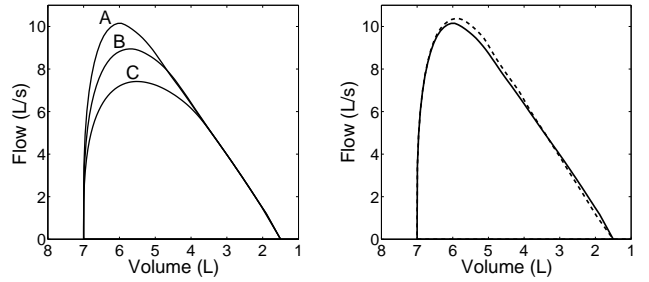


Figure 2: *Left*: Asymmetric tree: influence of patient's effort on flow-volume curves. A:  $P_m=24$  kPa and  $\tau=0.2$  s; B:  $P_m=18$  kPa and  $\tau=0.25$  s; C:  $P_m=12$  kPa and  $\tau=0.3$  s. *Right*: MEFV curves for the asymmetric (solid line) and symmetric (dashed line) trees.

We now investigate the behavior of altered bronchial trees under forced expiration. The chosen alteration is aging: it is modeled here by introducing a local modification of the mechanical properties of the small airways. A senile lung presents an increase of compliance that affects the smallest airways much more than the largest ones. The elastic recoil forces also decrease so that the smallest airways (which are the more compliant) are not completely open and tend to have a smaller maximal diameter [21]. Moreover, aging has also global effects on the lung behavior during forced expiration. Residual volume is increased [22] as well as tissue resistance [23]. The static recoil pressure depends also on age since the pulmonary compliance is increasing with age [24, 25]. Fig. 3 shows the MEFV curves computed for both symmetric and asymmetric senile lungs. Both structures present a reduced peak flow and a flow collapse after the peak flow as reported by Gibson et al. [26]

and Babb et al. [27]. However, the observed flow collapse is much larger in the symmetric case than in the asymmetric one. From a detailed examination of the flow distribution in the entire tree, it appears that the asymmetry creates airways of very different sizes at every generation which prevents the uniform collapse that occurs in the symmetric tree. Asymmetry therefore allows to better preserve the ventilation performances of the tracheobronchial tree even when the mechanical properties of the structure are altered.

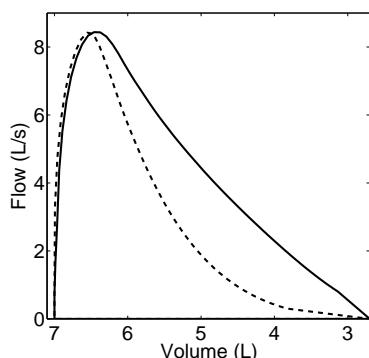


Figure 3: MEFV curves for asymmetric (solid line) and symmetric (dashed line) senile bronchial trees.

It has to be noted here that obstructive pathologies such as Chronic Obstructive Pulmonary Disease (COPD) or emphysema have very similar mechanical effects to those of aging. Therefore, it is very likely that the protective role of the branching asymmetry observed in the senile lung would also exist in these diseases.

## 5. Conclusion

In conclusion, the branching asymmetry measured in the human airway system appears to provide improved performance and robustness, both at inhalation and exhalation. At inhalation, the asymmetry provides robustness against anatomical variability. Moreover, using a simple ventilation model, we show that, in order to supply all acini with fresh air, the asymmetry level has to be smaller than 35%. Surprisingly, this happens to almost exactly correspond to the branching asymmetry measured in the human lung. At forced expiration, we developed a 1-D non linear compliant model that permits to compute the flow and pressure distributions in any bronchial tree, symmetric or asymmetric. By comparing MEFV curves, we show in this case that branching asymmetry improves the performance in senile or pathological lungs. From the point of view of evolution, one can therefore consider the asymmetry measured in the human airway system as optimal: it is large enough to provide a protection against obstructive pathologies at expiration, but not too large in order to preserve the oxygen supply at inhalation.

## References

[1] E. R. Weibel, *Morphometry of the Human Lung*, Springer Verlag / Academic Press, 1963.

[2] K. Horsfield, G. Cumming, *J. Appl. Physiol.* 24 (1968) 373–383.  
 [3] O. G. Raabe, H. C. Yeh, G. M. Schum, R. F. Phalen, *Tech. Rep. Publ. No. LF-53* (1976).  
 [4] A. Majumdar, A. M. Alencar, S. V. Buldyrev, Z. Hantos, K. R. Lutchen, H. E. Stanley, B. Suki, *Phys. Rev. Lett.* 95 (2005) 168101.  
 [5] K. Horsfield, G. Dart, D. E. Olson, G. F. Filley, G. Cumming, *J. Appl. Physiol.* 31 (1971) 207–217.  
 [6] C. G. Phillips, S. R. Kaye, *Resp. Physiol.* 102 (1995) 303–316.  
 [7] E. R. Weibel, *The Pathway for Oxygen, Structure and Function in the Mammalian Respiratory System*, Harvard University Press, Cambridge, 1984.  
 [8] E. R. Weibel, B. Sapoval, M. Filoche, *Resp. Physiol.* 148 (2005) 3–21.  
 [9] J. Sandeau, I. Katzb, R. Fodil, B. Louis, G. Apiou-Sbirlea, G. Caillibotte, D. Isabey, *J. Aero. Sci.* 41 (2010) 281–294.  
 [10] M. Filoche, A. A. Moreira, J. S. Andrade Jr., B. Sapoval, *Adv. Exp. Med. Biol.* 605 (2008) 167–72.  
 [11] B. Mauroy, M. Filoche, E. R. Weibel, B. Sapoval, *Nature* 427 (2004) 633–636.  
 [12] J. B. West, *Respiratory Physiology, The Essentials*, Eighth Edition, Lippincott Williams & Wilkins, 2008.  
 [13] R. K. Lambert, T. A. Wilson, R. E. Hyatt, J. R. Rodarte, *J. Appl. Physiol.* 52 (1982) 44–56.  
 [14] A. G. Polak, *Comput. Biol. Med.* 28 (1998) 613–625.  
 [15] D. Reynolds, *J. Biomech. Eng.* 104 (1982) 153–158.  
 [16] R. E. Hyatt, *J. Appl. Physiol.* 55 (1983) 1–8.  
 [17] S. V. Dawson, E. A. Elliott, *J. Appl. Physiol.* 43 (1977) 498–515.  
 [18] A. H. Shapiro, *Trans. ASME* (1977) 126–147.  
 [19] A. G. Polak, K. R. Lutchen, *Ann. Biomed. Eng.* 31 (2003) 891–907.  
 [20] P. Barbini, C. Brighenti, G. Cevenni, G. Gnudi, *Ann. Biomed. Eng.* 33 (2005) 518–530.  
 [21] H. Guenard, S. Rouatbi, *Rev. Mal. Respir.* 19 (2002) 230–240.  
 [22] J. Stocks, P. Quanjer, *Eur. Respir. J.* 8 (1995) 492–506.  
 [23] E. K. Verbeken, M. Cauberghs, I. Mertens, J. M. Lauweryns, K. P. V. de Woestijne, *J. Appl. Physiol.* 72 (1992) 2343–2353.  
 [24] E. K. Verbeken, M. Cauberghs, I. Mertens, J. Clement, J. M. Lauweryns, K. P. V. de Woestijne, *Chest* 101 (1992) 800–809.  
 [25] W. Galetke, C. Feier, T. Muth, K.-H. Ruehle, E. Borsch-Galetke, W. Randerath, *Respir. Med.* 101 (2007) 1783–1789.  
 [26] G. J. Gibson, N. B. Pride, C. O’Cain, R. Quagliato, *J. Appl. Physiol.* 41 (1976) 20–25.  
 [27] T. G. Babb, J. R. Rodarte, *J. Appl. Physiol.* 89 (2000) 505–511.